Available online at www.sciencedirect.com
SCIENCE DIRECT®
Journal of Magnetic Resonance 162 (2003) 90–101
JMR Journal of Magnetic Resonance
www.elsevier.com/locate/jmr

Carbon-13 lineshapes in solid-state NMR of labeled compounds. Effects of coherent CSA–dipolar cross-correlation

Luminita Duma,[a] Sabine Hediger,[a] Anne Lesage,[a] Dimitris Sakellariou,[b] and Lyndon Emsley[a,*]

[a] *Laboratoire de Stéréochimie et des Interactions Moléculaires (UMR-5532 CNRS/ENS), Laboratoire de Recherche Conventionné du CEA (23V), Ecole Normale Supérieure de Lyon, 69364 Lyon, France*
[b] *Department of Chemistry, University of California, Berkeley, CA 94720, USA*

Received 19 June 2002; revised 22 October 2002

Abstract

The experimental lineshapes of the carboxyl and methyl carbon resonances of fully ^{13}C enriched L-Alanine are studied in detail at different MAS frequencies and decoupling field strengths. Complex lineshapes at intermediate spinning speeds were explained by the *joint effect* of off rotational resonance and coherent CSA–dipolar cross-correlation. Whereas off rotational-resonance effects lead to complex lineshapes due to a splitting of some energy levels, coherent CSA–dipolar cross-correlation introduces either a differential intensity and/or a differential broadening of the lines of the *J*-multiplet. The conditions which lead to such effects are explained and experimentally verified. Additional simulations show that these effects can be expected over a wide range of static magnetic fields and are not restricted to L-Alanine.

1. Introduction

With the constant improvement of resolution in solid-state nuclear magnetic resonance (NMR), this technique is able nowadays to study larger molecular systems like proteins in a non-oriented environment [1–5]. This is mainly the result of technical improvement in high magnetic field, radio-frequency (RF) fields, magic-angle sample spinning (MAS), and sample preparation techniques. With these tools, in combination with sophisticated pulse sequences for decoupling and/or recoupling different interactions, an approach similar to that done in liquid-state NMR could be developed for the study of (non-oriented) biomolecules with solid-state NMR [4]. As in liquid-state NMR, most pulse sequences developed for this purpose are designed for fully labeled carbon-13 and nitrogen-15 molecules. The extensive use of carbon-13 labeling leads however to a broadening of the carbon lines due partly to the presence of the homonuclear *J*-couplings. When the resolution is good enough to resolve to some extent the fine structure due to the *J*-coupling, it was observed that this coupling does not necessarily induce the expected multiplet structure, but rather unusual broadened and asymmetric lineshapes [6,7], examples of which are given in Fig. 1. A better understanding of the different contributions that causes distorted and broadened lineshapes could enable the development of new techniques for enhancing the resolution in solid-state NMR. In this paper we will give a detailed explanation of which physical mechanisms lead to these lineshapes.

Several effects which have been described separately in literature must be invoked to explain these lineshapes. Broadening of the lineshape in a powder-pattern like fashion under MAS was already predicted in 1979 by Maricq and Waugh [8] for homonuclear coupled spin systems. Rotational-resonance effects [9–11] where the MAS frequency matches the difference of isotropic chemical shift of both nuclei must also be considered to explain complex lineshapes, even far from the exact rotational-resonance condition [12,13]. Finally, the interplay of the dipolar-interaction and chemical-shielding-

* Corresponding author. Fax: +33-4-72728483.
E-mail address: lyndon.emsley@ens-lyon.fr (L. Emsley).

1090-7807/03/$ - see front matter © 2003 Elsevier Science (USA). All rights reserved.
doi:10.1016/S1090-7807(02)00174-X

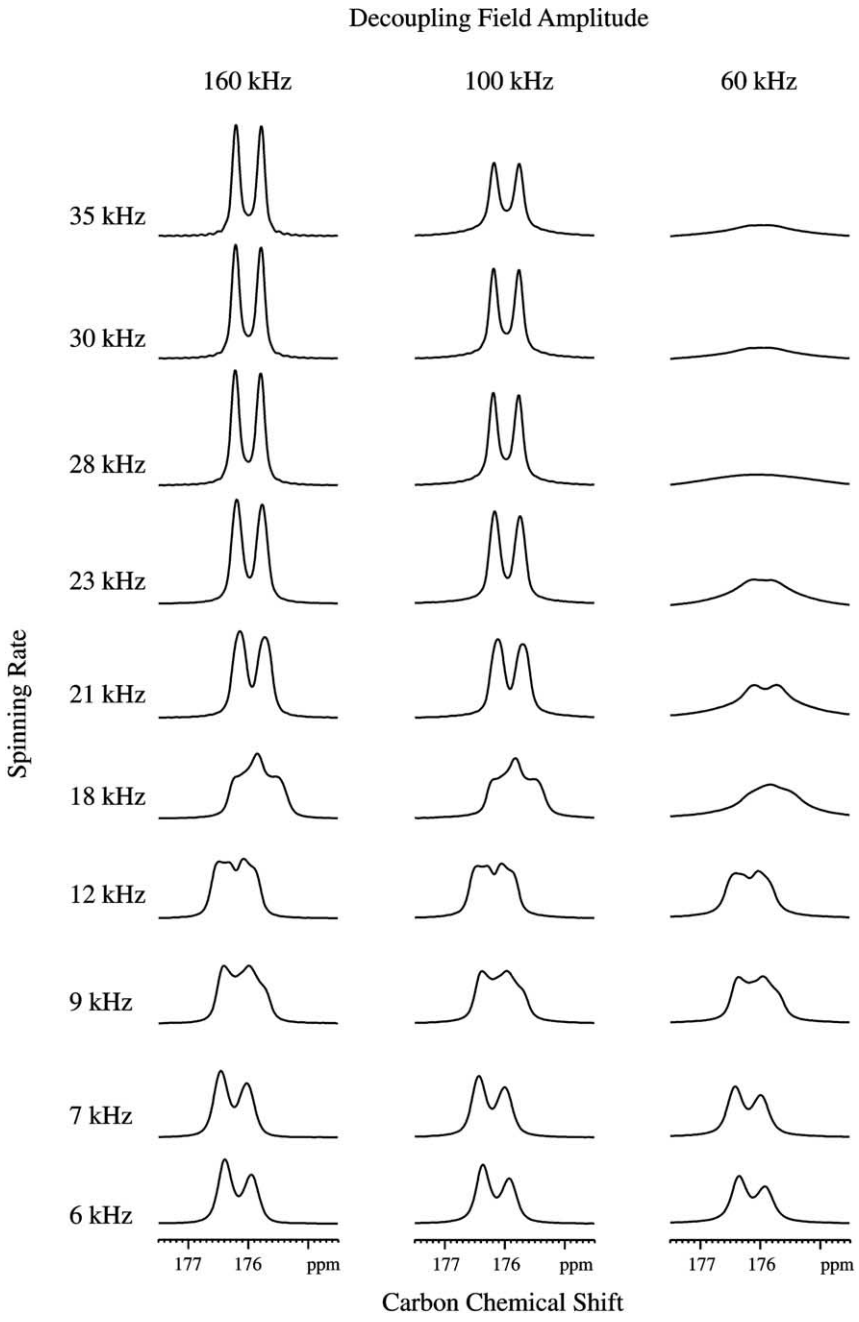

Fig. 1. Experimental carboxyl carbon lineshapes for 99% ^{13}C enriched L-Alanine at different spinning speeds and decoupling field strengths. The carbon spectra were obtained using the standard cross-polarization technique, with a ramped spin-lock on the proton channel to broaden the Hartman-Hahn condition [42–44]. The contact time was set to 1 ms. Detection was performed under TPPM decoupling [45]. To ensure the best resolution, the acquisition time was set to 60 ms, ensuring complete decay of the FID (at all spinning speeds). No exponential line broadening was applied.

anisotropy (CSA) tensors was shown to introduce an asymmetry in the intensity of the two peaks split by the isotropic coupling constant J in a heteronuclear two-spin system under slow sample spinning [14]. This kind of asymmetry was observed as well by Nakai and McDowell [15] in homonuclear spin-systems.

In this contribution we examine and discuss in more detail the specific experimental lineshapes observed for the carboxyl and the methyl carbons of ^{13}C enriched L-Alanine under a range of experimental conditions. By means of computer simulations, we show the relative impact of the different parts of the Hamiltonian on the spectral lineshape of a homonuclear coupled spin system. We show that in the case of a carboxyl carbon, the asymmetric powder lineshape can be explained by the *joint effect* of off rotational resonance [12,13] and a

coherent cross-correlation effect between the CSA of the carboxyl and the dipolar interaction between the carboxyl- and C_α-carbons, leading to an asymmetry in intensity between the two components of the multiplet [14,15]. For the methyl resonance in L-Alanine, a coherent cross-correlation effect is present as well, but is manifested this time additionally by a differential broadening of the doublet components. The conditions which lead to such distorted carbon lineshapes in homonuclear coupled spin-systems are discussed. Finally, we show with simulations that this situation is not restricted to the experimental conditions used here, but are expected for other compounds as well, and this over a wide range of magnetic fields.

In liquid state NMR, cross-correlation is a very well-known phenomenon, which manifests itself in the relaxation behavior of the spin system. The modulation by molecular motion of two different anisotropic spin interactions whose orientations are correlated (for example, the magnetic dipole–dipole interaction and the chemical shielding anisotropy) can give rise to this kind of relaxation process, generally called cross-correlated relaxation or cross-correlation (for reviews about that subject, see [16,17]). Such relaxation induced (incoherent) cross-correlation effects, which lead to a differential-line broadening of the *J*-multiplets, have also been seen in solids under MAS for compounds showing extensive molecular motion like liquid crystals or highly mobile solid polymers [18–21].

2. Experimental results

The experiments were all performed on a Bruker 500 Avance spectrometer (proton frequency at 500 MHz) equipped with a 2.5 mm double resonance CPMAS probe. All experiments were performed on 99% ^{13}C labeled L-Alanine purchased from Eurisotop and used without further purification. The carbon spectrum was measured for different MAS spinning frequencies (6, 7, 9, 12, 18, 21, 23, 28, 30, and 35 kHz) and decoupling field strengths (60, 100, and 160 kHz). Attention was paid in choosing the MAS frequencies that none of the carboxyl rotational-resonance conditions were matched. Considering that the isotropic chemical shift difference is 15.9 kHz between the COO^- (C') and CH (C_α) groups, and 19.8 kHz between the C' and CH_3 (C_β), the rotational-resonance conditions for the carboxyl carbon with the C_α resonance are at 5.3 ($n=3$), 8.0 ($n=2$), and 15.9 kHz ($n=1$), and at 6.6 ($n=3$), 9.9 ($n=2$), and 19.8 kHz ($n=1$) for the carboxyl with the C_β resonance. All chosen MAS frequencies are at least 1.2 kHz off the $n=1$ and 900 Hz off the $n=2$ rotational-resonance conditions. As the dipolar-coupling constant to the C_β is much smaller than to the C_α, off rotational-resonance effects from recoupling of the carboxyl resonance with the C_β are less important. The carboxyl resonance is shown in Fig. 1 for the different MAS frequencies at 60, 100 and 160 kHz decoupling field strengths.

Under high spinning speed and decoupling field, and well off rotational-resonance conditions, we expect the carboxyl resonance to be split into a symmetric doublet by the homonuclear *J*-coupling to the carbon C_α. Indeed, to zero order, the effect of the heteronuclear C–H dipolar coupling is removed by both MAS and decoupling, the heteronuclear C–H *J*-coupling is removed by decoupling, and the homonuclear carbon–carbon dipolar coupling by MAS, as long as rotational-resonance conditions are avoided. The effect of the carboxyl CSA should also be removed by MAS. However, the spectra of Fig. 1 show that the experimental lineshape is far from the expected symmetric doublet, except for spinning speeds well above 25 kHz. Below 9 kHz MAS and above 20 kHz, the lineshape looks like a more or less asymmetric doublet, with two components of different intensity but the same linewidth. This is especially marked at the lower MAS spinning speeds. In the lower spinning regime, broadening of the doublet was observed for the exact $n=3$ rotational-resonance condition at 5.3 kHz and 6.6 kHz MAS (not shown). However, off rotational-resonance effects from those conditions are small and appear negligible at 6 and 7 kHz. At 9, 12, and 18 kHz MAS, we obtain a powder-pattern like line, with a different shape at each spinning speed. It is difficult to follow more closely the change of the lineshape between these different spinning speeds, as rotational-resonance conditions would then be close to match, and their effects clearly dominate the lineshape. It is also noticeable that the center of gravity of the resonance moves slightly between 6 and 23 kHz, another effect of off rotational-resonance conditions [12,13].

The influence of the decoupling power on the lineshape is less drastic. Reduction of the decoupling power introduces a broadening of the lines due to less efficient decoupling of the protons, but the shape of the carboxyl line is not essentially modified. With a field strength of 60 kHz, the decoupling is not effective any more for spinning speeds higher than 20 kHz, reflecting probably the combined effect of less efficient decoupling and the onset of rotary-resonance recoupling, which is expected at 30 kHz MAS [22,23].

We do not show here in the same details the behavior of the CH (C_α) and CH_3 (C_β) carbon resonances of L-Alanine. The resolution of the CH resonance is not good enough to resolve the splitting due to the two *J*-couplings, and only a broad, featureless line is observed. In the case of the CH_3, the carbon resonance is better resolved than for the CH, and shows a more or less resolved doublet structure at all MAS frequencies that are not too close to rotational resonance conditions. At the lower spinning speeds, however, an asymmetry in the

line intensities and widths of the doublet leads us to suspect similar effects on the methyl lineshape as those observed for the carboxyl, as will be discussed in detail below.

The effects on the lineshape that we describe here seem to be a general problem in fully ^{13}C labeled samples. Unexpected lineshapes were indeed also observed in carbon spectra of fully labeled proteins [3,7,24]. As an example, in the spectrum of the α-spectrin SH3 domain measured at a field of 17.6 T and published in Fig. 2a of [3], the resolved resonances of Val53 C_γ at 17.0 ppm and Ala55 C_β at 15.9 ppm are obviously asymmetrically broadened (for the carbon assignment, see [4]).

3. Theoretical aspects and simulations

The theory concerning the different aspects considered in this contribution has already been treated in the literature individually. However, in order to separate the different contributions to the lineshape and understand the experimental observations, we will recall here a broad outline of the theory.

Let us first consider the case of a static sample. The Hamiltonian of a static two-spin system in the rotating frame of the Zeeman interaction is given by the following expression:

$$H = H_{\mathrm{iso}} + H_{\mathrm{CSA}} + H_{\mathrm{D}} + H_J \tag{1}$$

with H_{iso} the isotropic chemical shift of both spins I and S, H_{CSA} the anisotropic part of the chemical shift which is here only considered for the spin I, H_{dip} the dipolar interaction between both spins, and H_J the scalar J-coupling:

$$\begin{aligned} H_{\mathrm{iso}} &= \omega_{0I} I_z + \omega_{0S} S_z, \\ H_{\mathrm{CSA}} &= \omega_{\mathrm{CSA}}(\Omega) I_z, \\ H_{\mathrm{D}} &= \omega_{\mathrm{D}}(\Omega')(3I_zS_z - I\cdot S) = \omega_{\mathrm{D}}(\Omega')(2I_zS_z - I_xS_x - I_yS_y), \\ H_J &= \pi J 2 I_z S_z, \end{aligned} \tag{2}$$

where Ω and Ω' represent the two sets of Euler angles connecting the principal axis systems of the CSA and dipolar tensors, respectively, to the crystallite orientation in the laboratory frame. The relation between Ω and Ω' depends on the geometry of the spin system. In matrix form, this Hamiltonian is given by:

$$H = \frac{1}{2}\begin{pmatrix} \omega_{0I}+\omega_{0S}+\pi J+\omega_{\mathrm{CSA}}+\omega_{\mathrm{D}} & 0 & 0 & 0 \\ 0 & \omega_{0I}-\omega_{0S}-\pi J+\omega_{\mathrm{CSA}}-\omega_{\mathrm{D}} & -\omega_{\mathrm{D}} & 0 \\ 0 & -\omega_{\mathrm{D}} & -\omega_{0I}+\omega_{0S}-\pi J-\omega_{\mathrm{CSA}}-\omega_{\mathrm{D}} & 0 \\ 0 & 0 & 0 & -\omega_{0I}-\omega_{0S}+\pi J-\omega_{\mathrm{CSA}}+\omega_{\mathrm{D}} \end{pmatrix}, \tag{3}$$

where the elements of the basis are: $|1\rangle = |\alpha,\alpha\rangle$, $|2\rangle = |\alpha,\beta\rangle$, $|3\rangle = |\beta,\alpha\rangle$, and $|4\rangle = |\beta,\beta\rangle$, the first symbol representing the state of the I spin and the second one of the S spin.

Let us now consider that the isotropic chemical shift difference is larger than all the other interactions (which is for example always the case in heteronuclear spin systems in the high magnetic field approximation). In this case, the off-diagonal elements of this matrix can be considered as non-secular and can be neglected. The two single-quantum transitions for the I spin appear at the frequencies:

$$\begin{aligned} \omega_{\alpha\alpha\to\beta\alpha} &= \omega_{0I} + \pi J + \omega_{\mathrm{CSA}}(\Omega) + \omega_{\mathrm{D}}(\Omega'), \\ \omega_{\alpha\beta\to\beta\beta} &= \omega_{0I} - \pi J + \omega_{\mathrm{CSA}}(\Omega) - \omega_{\mathrm{D}}(\Omega'). \end{aligned} \tag{4}$$

The two transitions which are separated by the J-coupling have a powder lineshape due to the orientation-dependent contributions of the CSA and dipolar terms. However, due to the fixed relative orientation of both tensors, the contribution of the two terms are "added" for one transition and "subtracted" for the other one. This leads to powder patterns of different shapes and widths for the two transitions of the I spin. The difference in width of the powder patterns depends on the relative size and orientation of the CSA and the dipolar tensors. A detailed analysis of the pattern of both transitions can be found in [25]. In a homonuclear spin-system, the off-diagonal elements of Eq. (3) introduce an additional term to the resonance frequencies of Eq. (4), which depends non-linearly on ω_{D} and ω_{CSA}. However, this term is the same for both transitions. Differential linewidths of the resonance components will therefore still be expected from the relative contribution of CSA and dipolar terms which are added for one transition and subtracted for the other. This is illustrated in Fig. 2 where simulations of the I spin transitions in the static case are shown. In Fig. 2a the geometry of L-Alanine was considered with the I spin representing the carboxyl and the S spin the C_α. It is clear in this simulation that the first carboxyl transition $\alpha\alpha \to \beta\alpha$, e.g. with the C_α in α-state, is broader than the second transition $\alpha\beta \to \beta\beta$ with C_α in β-state. Since only the I spin signal is shown in Fig. 2a for reasons of clarity, a small dispersive signal appears at the chemical shift of the S spin due to the mixing of the spin-states by the off-diagonal elements of Eq. (3), which are not completely non-secular in this homonuclear spin system. In Fig. 2b the I spin represents the C_β of L-Alanine coupled to the C_α (S spin). Here again, the difference in width of both components

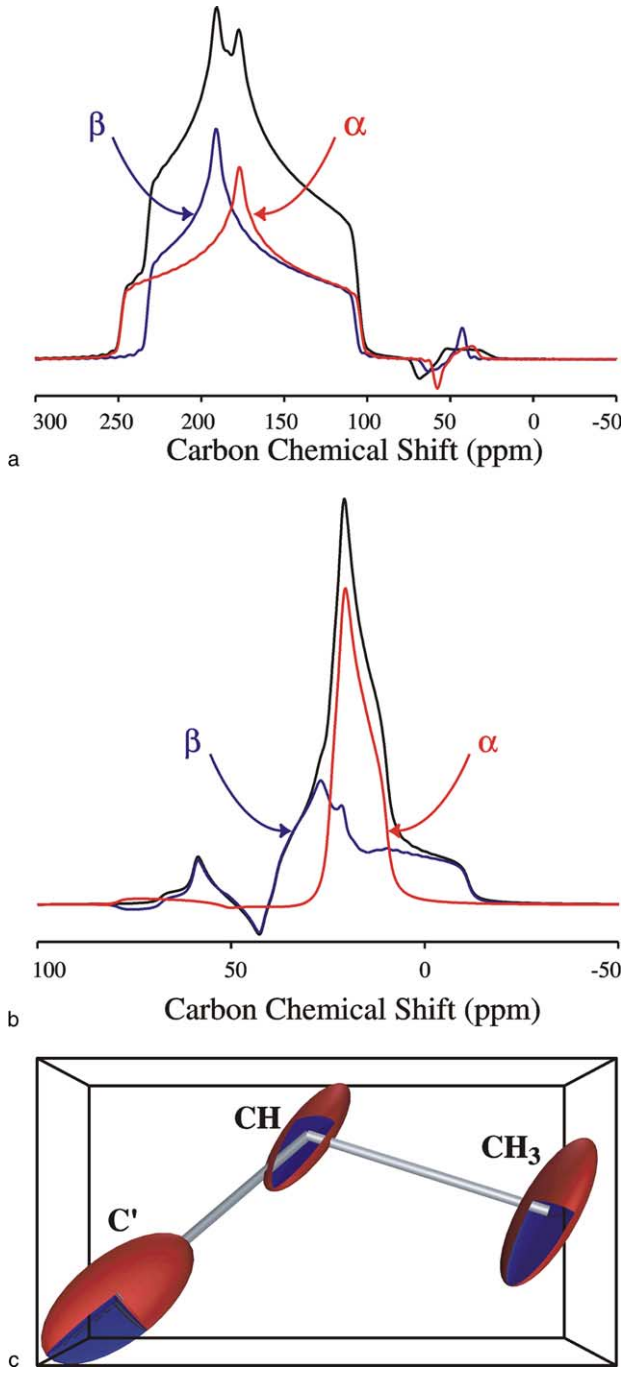

Fig. 2. Simulated static powder pattern for the (a) C′ and (b) C_β in L-Alanine. For the carboxyl, the transition $\alpha\alpha \rightarrow \beta\alpha$, e.g. with C_α in α state, is broader than the transition $\alpha\beta \rightarrow \beta\beta$ with the C_β in β state. Regarding the methyl, the transition $\alpha\alpha \rightarrow \beta\alpha$ is narrower than the transition $\alpha\beta \rightarrow \beta\beta$. For both simulations, the system was reduced to two spins under the Hamiltonian of Eqs. (1) and (2), the S spin being in both cases the C_α. The different parameters for the CSA and dipolar tensors, as well as their relative orientation are given in Table 1. In both cases, the CSA of the S spin was neglected. The $^1J_{C'C_\alpha}$ and $^1J_{C_\beta C_\alpha}$ scalar couplings were set to 54 and 34 Hz, respectively. A planar grid powder average over 1,000,000 different crystal orientations was performed to obtain the simulated powder spectra [32]. These simulations were obtained using Matlab [33]. (c) Geometry of the CSA and dipolar tensors with respect to the molecular frame, for all carbons in L-Alanine. This picture was obtained using SIMMOL package [26].

is evident, whereby the relative orientation of the C_β-CSA and the dipolar coupling lead this time to a broader pattern for the transition with C_α in β-state ($\alpha\beta \rightarrow \beta\beta$). The geometry of all the tensors with respect to the molecular frame is given in Fig. 2c using the SIMMOL package [26]. The exact values considered for the different CSA tensors and the dipolar interaction were taken or calculated from [27–29] and are summarized in Table 1.

In the static case, the correlated effect of the CSA- and dipolar tensors appears directly to zero order in the Hamiltonian, leading for the I spin to two transitions of different shape. The introduction of sample spinning will affect identically both transitions. The Hamiltonian of Eq. (1) becomes in this case time-dependent

$$H(t) = H_{\mathrm{iso}} + H_{\mathrm{CSA}}(\Omega, t) + H_{\mathrm{D}}(\Omega', t) + H_J \tag{5}$$

with the time-dependent terms:

$$\begin{aligned} H_{\mathrm{CSA}}(\Omega, t) &= \omega_{\mathrm{CSA}}(\Omega, t) I_z, \\ H_{\mathrm{D}}(\Omega', t) &= \omega_{\mathrm{D}}(\Omega', t)(2I_z S_z - I_x S_x - I_y S_y). \end{aligned} \tag{6}$$

Let us now consider two situations, depending upon whether the Hamiltonian behaves homogeneously or not.

3.1. The inhomogeneous case

If the secular approximation made above is valid, the dipolar contribution in Eq. (6) can be reduced to its $I_z S_z$ component, and the Hamiltonian then commutes with itself at any time during the rotation. In such a situation, the spin system is considered to behave inhomogeneously in the sense of Maricq and Waugh [8]. Spinning at the magic angle will lead to a perfect refocusing of the anisotropic part of the magnetization at integer multiples of the rotor period, leading to two well-resolved spinning sideband manifolds, one for each transition of the I spin. The static powder pattern of these two transitions being however different from each other, with for instance different widths, the sideband manifolds for each transition will be different. An *asymmetry in intensity* between both central transitions will therefore normally be present for spinning speeds lower than the static transition width, with the most intense line belonging to the transition with the narrowest static pattern. This was indeed already observed for an heteronuclear spin system by Harris et al. [14], where both sideband manifolds corresponding to the two transitions of a carbon coupled to a phosphorous had different intensities at slow spinning speeds, resulting directly from the difference in shape of the two transitions in the static case. It was also observed by Nakai and McDowell [15] in a homonuclear two-spin system with a large difference in isotropic chemical shifts (doubly ^{13}C labeled sodium acetate).

We see here in the case of the carboxyl of fully enriched L-Alanine that this effect of coherent cross-cor-

Table 1
Parameters for the carbon CSA tensors, *J*-coupling and dipolar tensors in L-Alanine

CSA parameters	$^{13}C'$	$^{13}C_\alpha$	$^{13}C_\beta$
$\omega_{iso}/2\pi$[a]	176 ppm	50 ppm	19 ppm
$\omega_{aniso}/2\pi$[b]	−70 ppm	−20 ppm	−12 ppm
η[b]	0.78	0.32	1
Ω_{PM}[c]	(11.7°, 86.3°, −53°)	(81.7°, 24.5°, 29.1°)	(52.9°, 77.4°, 140.5°)
Scalar and dipolar couplings parameters	$^{13}C'$–$^{13}C_\alpha$	$^{13}C'$–$^{13}C_\beta$	$^{13}C_\alpha$–$^{13}C_\beta$
J_{jk}[d]	54 Hz	0 Hz	34 Hz
$d_{jk}/2\pi$[e]	−2092.5 Hz	−474.76 Hz	−2104.8 Hz
Ω'_{PM}[c]	(0°, 21.5°, −154°)	(0°, 46.6°, 160.4°)	(0°, 78.4°, 144.7°)

[a] Isotropic chemical shifts from [28] with respect to TMS.
[b] $\omega_{aniso} = \omega_0(\delta_{zz} - \delta_{iso})$, $\eta = (\delta_{yy} - \delta_{xx})/(\delta_{zz} - \delta_{iso})$, with the chemical shielding principal values taken from [28] and ordered as following: $|\delta_{zz} - \delta_{iso}| \geqslant |\delta_{xx} - \delta_{iso}| \geqslant |\delta_{yy} - \delta_{iso}|$.
[c] Set of Euler angles from [29] between the principal axis system of the tensors and the crystallographic reference frame [27].
[d] Measured in a liquid state NMR spectrum of ^{13}C enriched L-Alanine.
[e] $d_{jk} = -\mu_0\gamma^2\hbar/4\pi r_{jk}^3$, with the internuclear distances r_{jk} from [39].

relation between a CSA and a dipolar tensor is expected in a fully labeled amino acid. Indeed the chemical shift difference between C' and C_α is large enough for this homonuclear two-spin system to behave inhomogeneously. Fig. 3 compares the experimental lineshape of the carboxyl resonance of fully ^{13}C labeled L-Alanine with numerical simulations. The same two-spin C'–C_α system was considered as for the static simulations including the C'–C_α dipolar interaction and the CSA of only the C'. The asymmetry in the line intensities of the doublet is very clear at 6 and 7 kHz MAS, and remarkably well predicted by the simulations, despite the two-spin approximation and the omission of the C_α CSA. Only at spinning speeds higher than the width of the static spectrum (above 20 kHz), the CSA–dipolar terms are fully averaged and the whole spectral intensity concentrated in the centerband for each transition, leading to a symmetric doublet.

At intermediate spinning speeds, the lines are additionally broadened by so called off rotational-resonance effects. This broadening mechanism was extensively discussed by Levitt et al. [12] and Nakai and McDowell [13]. When the MAS spinning speed comes close to a rotational-resonance condition, $|\omega_{0I} - \omega_{0S}| \cong n\omega_r$ with n a small integer, the non-secular time-dependent off-diagonal elements of Eq. (3) contain a component which starts to be resonant with the energy levels $|\alpha,\beta\rangle$ and $|\beta,\alpha\rangle$. This induces a splitting of each of these two levels into a pair of time-independent virtual states, leading to a splitting of all single-quantum resonances [12]. The single-quantum spectrum of the I spin is no longer made up of two components (see Eq. (4)) but four for each crystallite orientation. As the splitting depends on the dipolar coupling and thus the crystallite orientation, experimental conditions at or close rotational resonance lead to complex powder lineshapes.

At exact rotational resonance, the broadenings can be several hundred Hertz. Although they drop off rapidly away from match, they can still be relevant to the lineshapes we observe, where the dominant interactions are only a few tens of Hertz. Indeed, in the case of the carboxyl resonance in L-Alanine, this phenomenon dominates the lineshape for spinning speeds between 9 and 20 kHz (see Fig. 3). The different powder shapes are again extremely well predicted with the numerical simulations of the two-spin system given in the middle column of Fig. 3. The separate simulations of the two *J*-components $\omega_{\alpha\alpha\to\beta\alpha}$ and $\omega_{\alpha\beta\to\beta\beta}$ clearly show the splitting due to broad rotational-resonance effects. It is worth noting that these two *J*-components have the same lineshape: the off rotational-resonance effects act in the same way on both transitions. The intensity of the two broadened transitions may however differ due to the coherent cross-correlation between CSA and dipolar interactions described above. This is particularly noticeable at 9 and 12 kHz, where the simulations including the carboxyl CSA match very well the experimental lineshapes, and clearly show two resonances of different intensity. The simulations without CSA (right column of Fig. 3) exhibit as expected two identical transitions split by the *J*-coupling.

3.2. The homogeneous case

If the chemical shift difference between both spins I and S is comparable to the dipolar interaction, the system behaves under MAS homogeneously [8]. In that case, the Hamiltonian does not commute with itself at all times, and MAS only partly refocuses the anisotropic component at multiples of the rotor period. The *linewidth* therefore now depends on the MAS frequency, with the resolution improving with increasing spinning speed. In that case, we expect coherent CSA–dipolar cross-correlation to lead to a *differential broadening* of both lines in the doublet. Indeed for a given MAS frequency, the narrower static transition will be better averaged and therefore narrower than the broader transition. This effect will of course decrease with

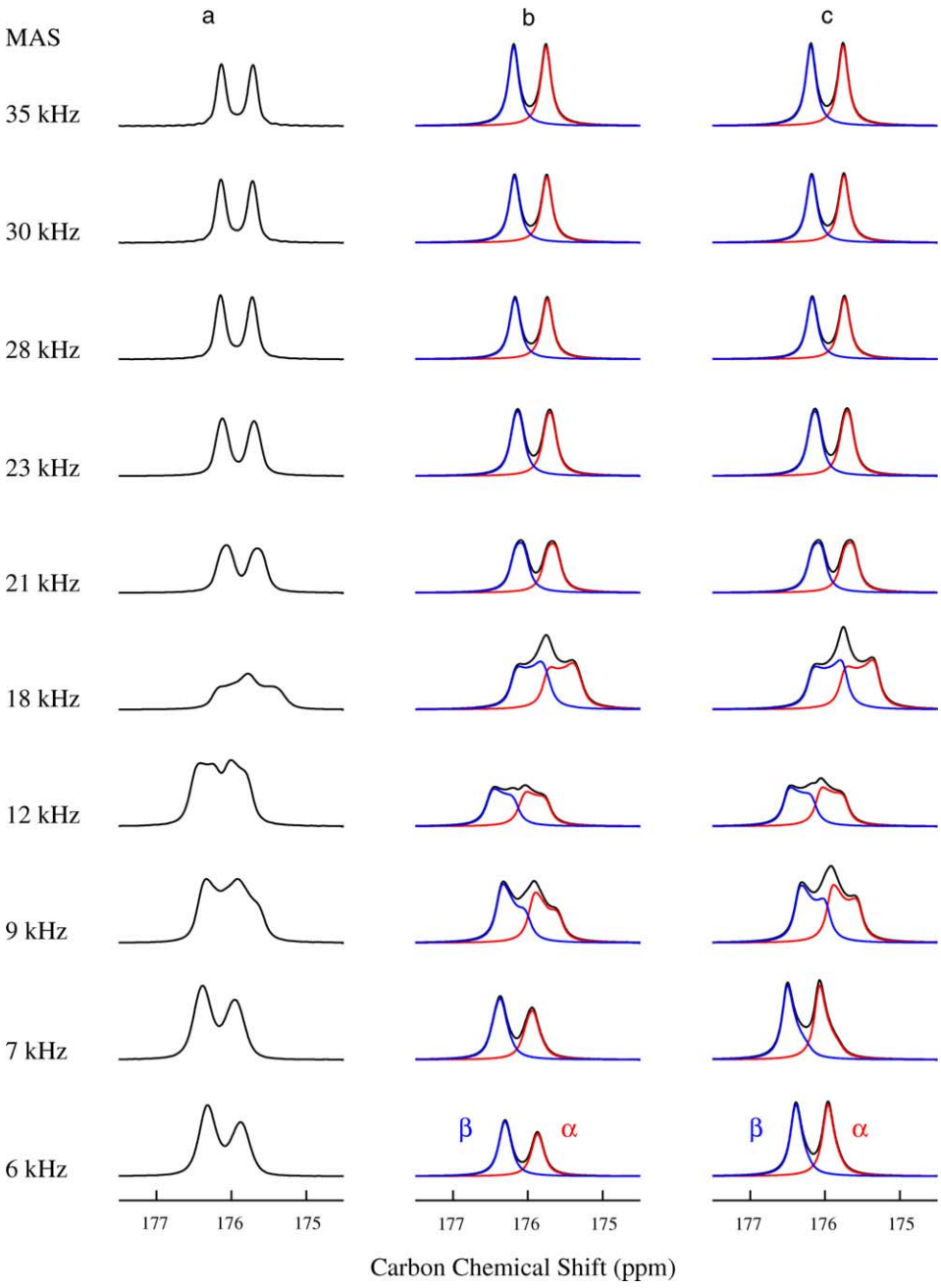

Fig. 3. Comparison of (a) the experimental lineshape of the carboxyl resonance of L-Alanine at different spinning speeds with (b–c) numerical simulations. The experimental spectra are those measured with 160 kHz decoupling field strength (see Fig. 1 for experimental details). For the simulations, the same spin system was considered as for the static simulation of Fig. 2a. In the simulations of column (c), the CSA part of the Hamiltonian ($H_{CSA} = \omega_{CSA}(\Omega, t)I_z$) was omitted. For all the simulated spectra, a ZCW powder average over 62,700 different crystal orientations was performed [32]. The simulations were obtained with the NMR simulation package SIMPSON [31]. A line broadening of 24 Hz was applied prior to Fourier Transform.

increasing spinning speed. The expectation of differential broadening in the multiplet structure of a homonuclear spin system under MAS was mentioned by Maricq and Waugh [8], but to our knowledge no experimental evidence for this effect has been previously observed.

Inspecting the CH_3 carbon resonance in fully ^{13}C enriched L-Alanine, shown in Fig. 4a, demonstrates this kind of differential broadening. Between 7 and 12 kHz MAS, the doublet due to the *J*-coupling to the C_α starts to be resolved. Deconvolution of this doublet reveals components of different widths, with the downfield component (C_α in the β-state) being wider (see Fig. 4b). The differential broadening decreases as expected with the MAS frequency, going in our case from approximately 6 Hz at 7 kHz MAS (an effect of 15%) to 3 Hz at

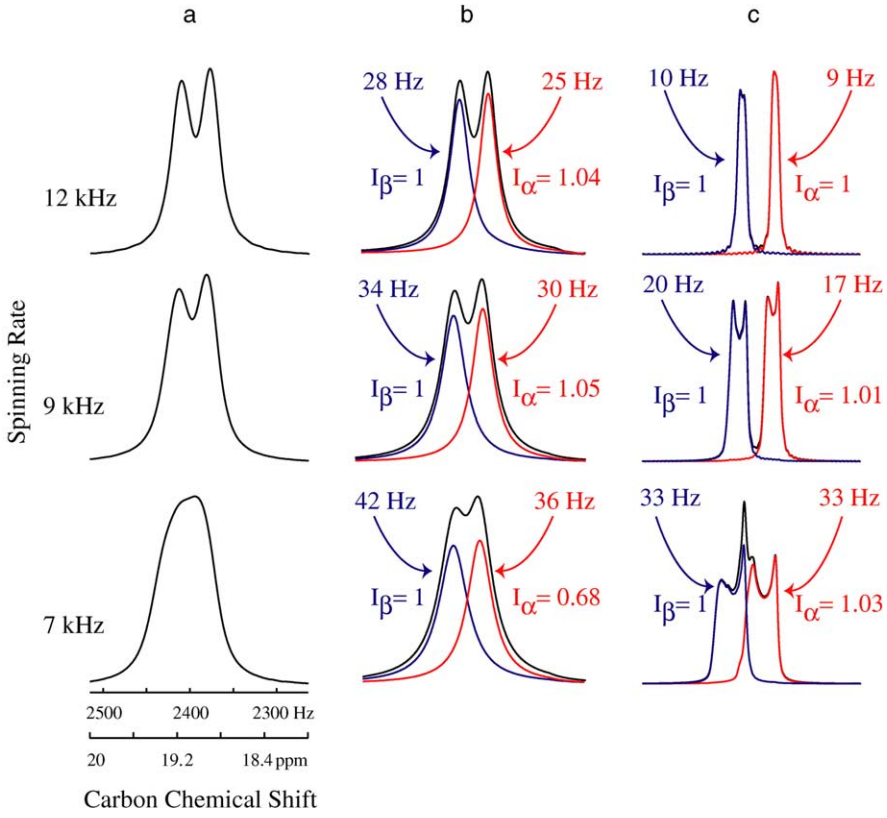

Fig. 4. (a) Experimental lineshape of the C_β resonance of L-Alanine at different spinning speeds with a 160 kHz decoupling field strength. Experimental details are given in the caption of Fig. 1. No linebroadening was applied prior to Fourier Transform. Each experimental line was deconvoluted with two Lorentzian functions. The result of the deconvolution is given in (b), with the Lorentzian linewidth at half height and integral over each component (*I*). (c) Simulations under magic angle spinning for the C_β in L-Alanine. To simulate the differential linebroadening for the methyl, the dipolar couplings to a third spin are necessary, here C′ was considered [30]. A ZCW powder average over 62,700 different crystal orientations was performed to obtain the simulated spectra [32]. The simulations were obtained with the NMR simulation package SIMPSON [31]. A small line broadening (3 Hz) was applied prior to Fourier Transform to smooth down the lines.

12 kHz MAS. Increasing further the spinning speed leads to a symmetric doublet (within the limit of uncertainty of the measurement). We should note that the difference in linewidth also leads to a different intensity for the two components. However, the integrated intensity over both deconvoluted components is the same in all the spectra (except at 7 kHz MAS, for which spectrum we could not obtain a good deconvolution). This indicates that the inhomogeneous contribution to the lineshape is very small here. The difference in intensity arises therefore only from the differential broadening, and not from differences in spinning sidebands intensity distribution, as it is the case for the carboxyl resonance (inhomogeneous interactions).

We have tried to simulate the differential broadening induced by coherent cross-correlation using the tensor geometry found in L-Alanine. Interestingly, it was impossible to obtain components of significantly different width with only two spins (C_β and C_α), even by considering both CSAs, and modifying the tensor parameters to force the system to behave as homogeneously as possible. A difference in width of the two components of the doublet was obtained only when dipolar couplings to a third spin (C′) were introduced. This is in agreement with Filip et al. [30] who claim that the lineshape of homogeneous system is dominated at lower spinning speed by three-spin (and higher) terms. Only at higher spinning speeds do these terms get smaller, and the lineshape can be explained using a spin-pair approximation.

Simulations of the C_β resonance of L-Alanine are given in Fig. 4c. The *J*-coupling between C_β and C_α, all the dipolar couplings between the three spins in one molecule of L-Alanine and CSA of C_β were taken into account. The simulated spectra which are shown with a small line broadening (LB = 3 Hz) do not reproduce exactly the experimental spectra. This is not too surprising, since homogeneous spin systems are notoriously difficult to simulate accurately, and it is probable that more spins need to be added to the simulation to reproduce the experimental spectra accurately. However, what is most important to note is that the simulations do predict different lineshapes and widths for the two transitions, in contrast to the inhomogeneous simulations of Fig. 3. Of course, off rotational-resonance

effects will also additionally affect the lineshape in the homogeneous case. For the particular case of the CH_3 in L-Alanine shown here, the MAS frequencies were chosen such that off rotational-resonance effects were negligible.

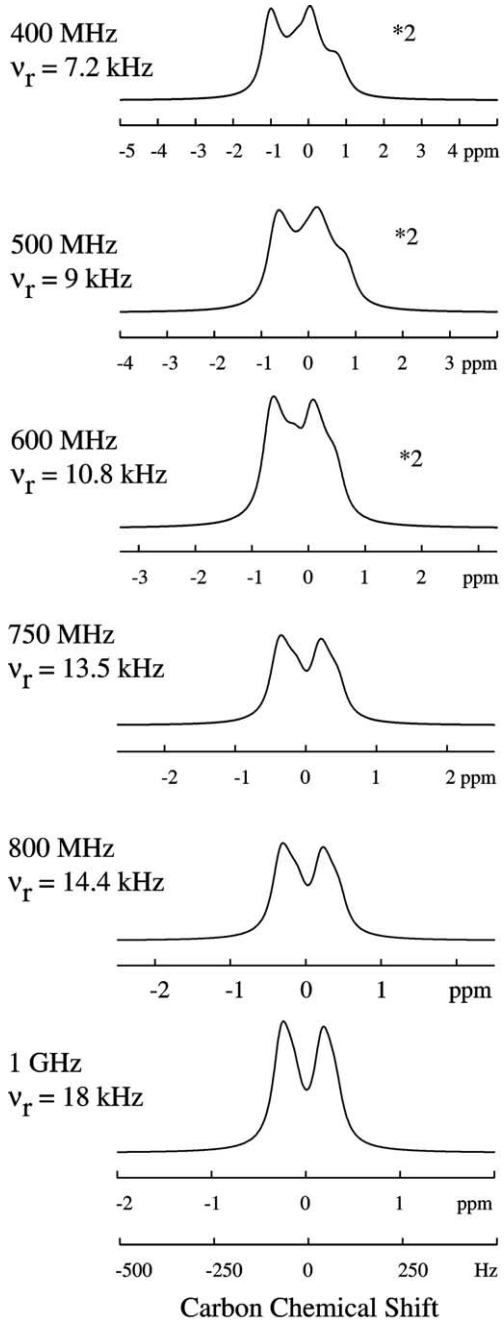

Fig. 5. Simulations under magic angle spinning of the carboxyl resonance of L-Alanine at different static magnetic fields ranging from 400 MHz to 1 GHz proton frequency. The spinning frequency was chosen such that its ratio to the magnetic field was kept constant. The same spin system was considered as for the static simulation of Fig. 2a. A ZCW powder average over 5640 different crystal orientations was performed to get the simulated spectra [32]. The simulations were obtained with the NMR simulation package SIMPSON [31]. A line broadening of 24 Hz was applied prior to Fourier Transform.

All simulations under MAS were performed with the NMR simulation package SIMPSON [31] using standard methods [32]. The static simulations as well as the deconvolution of the CH_3 resonance of L-Alanine (see Fig. 4) were obtained using Matlab [33].

4. Discussion

Our results show that the experimental lineshape observed for fully labeled L-Alanine can be explained by the joint effect of off rotational-resonance conditions and cross-correlation between the CSA and dipolar interactions. Such effects are however not limited to the special case considered in detail here, but also appear *at other magnetic fields or in other amino acids*, and are therefore relevant for all ^{13}C labeled samples.

To illustrate this, in Fig. 5, the lineshape of the carboxyl resonance of L-Alanine is simulated for a series of different static magnetic fields corresponding to 400 MHz to 1 GHz proton resonance frequencies. To keep the size of the off rotational-resonance effects constant, the MAS frequency was adjusted such that its ratio to the magnetic field remained the same for all simulated spectra. Even if the distortion of the lineshape from the expected symmetric doublet tends to be smaller at higher magnetic fields, it still leads to noticeable effects at 800 MHz proton frequency. We predict therefore

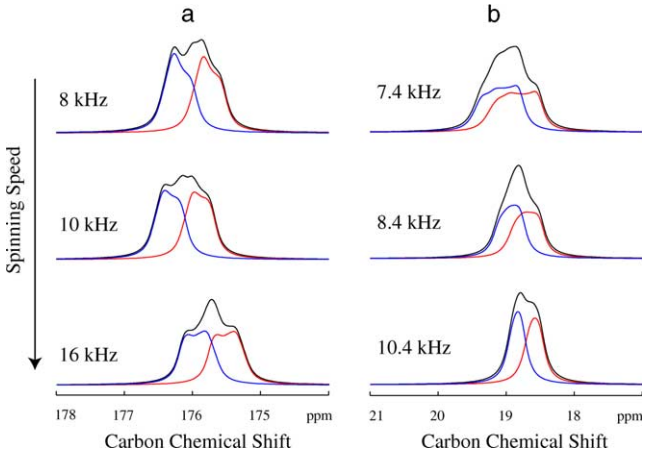

Fig. 6. Simulated (a) carboxyl and (b) methyl resonances for L-Threonine at intermediate spinning speeds and 500 MHz proton frequency. The different parameters for the CSA and dipolar tensors, as well as their relative orientations are given in Table 2. For the simulations of the carboxyl (C′) lineshape a two spin-system C′–C_α was considered. Only the CSA of the carboxyl spin was taken into account. For the methyl (C_δ) lineshape simulations, a four spin-system C′–C_α–C_β–C_γ was chosen. All CSA tensors and dipolar couplings between all four spins were considered. The parameters for the different interactions are given in Table 2. A ZCW powder average over 5640 different crystal orientations was performed to obtain the simulated spectra [32]. The simulations were obtained with the NMR simulation package SIMPSON [31]. A line broadening of 24 Hz was applied prior to Fourier Transform.

Table 2
Parameters for the carbon CSA tensors, *J*-coupling and dipolar tensors in L-Threonine

CSA parameters	$^{13}C'$	$^{13}C_\alpha$	$^{13}C_\beta$	$^{13}C_\gamma$	
$\omega_{iso}/2\pi$[a]	170 ppm	60.2 ppm	65.4 ppm	18.9 ppm	
$\omega_{aniso}/2\pi$[b]	70.2 ppm	8.8 ppm	−26.6 ppm	−17.5 ppm	
η[b]	0.85	0.71	0.35	0.51	
Ω_{PM}[c]	(83.7°, 69.4°, 154.4°)	(149°, 58.3°, 88.7°)	(50°, 110.4°, 150.9°)	(1.7°, 147°, 72.8°)	
Scalar and dipolar couplings parameters	$^{13}C'$–$^{13}C_\alpha$	$^{13}C'$–$^{13}C_\beta$	$^{13}C_\alpha$–$^{13}C_\beta$	$^{13}C_\alpha$–$^{13}C_\gamma$	$^{13}C_\gamma$–$^{13}C_\beta$
J_{jk}	54 Hz	0 Hz	34 Hz	0 Hz	34 Hz
$d_{jk}/2\pi$[d]	−2176.5 Hz	−454.5 Hz	−2072.3 Hz	−467 Hz	−2229 Hz
Ω'_{PM}[c]	(0°, 126.8°, 147.7°)	(0°, 125.2°, 18.6°)	(0°, 104.3°, 59.2°)	(0°, 50.4°, 64.5°)	(0°, 20.9°, 73.3°)

[a] Isotropic chemical shifts calculated from [40] with respect to TMS.
[b] $\omega_{aniso} = \omega_0(\delta_{zz} - \delta_{iso})$, $\eta = (\delta_{yy} - \delta_{xx})/(\delta_{zz} - \delta_{iso})$, with the chemical shielding principal values estimated from [40] and ordered as following: $|\delta_{zz} - \delta_{iso}| \geqslant |\delta_{xx} - \delta_{iso}| \geqslant |\delta_{yy} - \delta_{iso}|$.
[c] Set of Euler angles between the principal axis system of the tensors and the crystallographic reference frame, determined from the atomic parameters given in [41].
[d] $d_{jk} = -\mu_0\gamma^2\hbar/4\pi r_{jk}^3$, with the internuclear distances r_{jk} from [41].

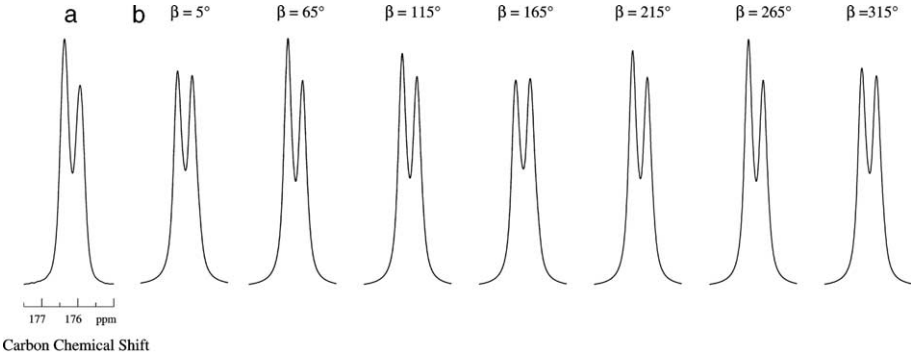

Fig. 7. (a) Experimental C′ lineshape at 7 kHz spinning rate, taken from Fig. 1. (b) Simulations similar to Fig. 3, but varying the angle β between the z-component of the C′ CSA tensor and the C′–C_α internuclear vector, showing the sensitivity of the lineshape to this structurally relevant parameter. The simulations of Fig. 3 were done for $\beta = 64.8°$, swhich is the value found from [39].

that cross-correlation and off rotational-resonance effects can broaden the carbon resonances of fully ^{13}C labeled proteins, even at the highest available magnetic field strengths. The asymmetric lineshapes observed in [3] for the SH3 domain resonances C_γ of Val53 (17.0 ppm) and C_β of Ala55 (15.9 ppm) are good examples of this.

To illustrate the generality of this effect with respect to the spin system, we have simulated the lineshapes of resonances using the parameters for the carboxyl and methyl groups of L-Threonine for different MAS spinning speeds (see Fig. 6, and Table 2 for the size and geometry of the different interactions). The broadening of these simulated lines is seen in Fig. 6 to be quite similar to that described above for L-Alanine.

As was briefly mentioned by Nakai and McDowell [15], we note that the coherent cross-correlation effect we observe for carbon lineshapes could potentially be used to determine the orientation of the CSA tensor in the molecular frame, if the principle components are known (or vice-versa). This is illustrated in Fig. 7 where we show the predicted lineshape of the C′ carbon in L-Alanine as a function of the angle β between the z-component of the CSA tensor and the C′–C_α internuclear vector. The change is clear, and only the previously determined geometry of the Table 1 agrees with the experimental result.

5. Conclusions

We have shown that carbon-13 spectra of fully labeled compounds can reveal at intermediate spinning speeds broadened and asymmetric lineshapes instead of the expected multiplet structure due to the scalar couplings. Whereas the broadening of the lines originates mainly from well-known off rotational-resonance effects, coherent CSA–dipolar cross-correlation was shown to induce an asymmetry in intensity for inhomogeneous systems [13,14], and this will be the case for the vast

majority of carboxyl resonances in proteins for example. In homogeneous systems, coherent cross-correlation effects were shown to induce differential broadening for the first time. This will be the case, for example, for many aliphatic groups in proteins. The effect we describe here is widespread *and is particularly relevant for solid-state NMR studies of proteins*, where current experimental practice favors the use of intermediate spinning speeds that appear to maximize these effects, and we show that these effects are still noticeable at the highest available magnetic fields.

In all cases these coherent cross-correlation effects disappear at high spinning frequencies. At low spinning rates, the coherent cross-correlation effects in carbon-13 labeled systems can be eliminated by selective pulses which refocus the homonuclear *J*-coupling in experiments such as those proposed by Straus et al. [34]. Indeed, Igumenova and McDermott [35] have recently been working towards experiments specifically aimed at removing these effects.

Finally, cross-correlation effects in liquid state NMR have successfully been exploited as sensitive structural probes [36,37] and differential broadening has recently been exploited in the TROSY experiment [38] to yield resolution enhancement in spectroscopy of proteins. It is conceivable that the exploitation of these effects in solids could also lead to new, unexpected applications.

Acknowledgments

The authors thank Prof. Jay H. Baltisberger (Berea) for very stimulating discussions.

References

[1] S.K. Straus, T. Bremi, R.R. Ernst, Experiments and strategies for the assignment of fully C-13/N-15-labelled polypeptides by solid state NMR, J. Biomol. NMR 12 (1998) 39–50.

[2] A. McDermott, T. Polenova, A. Böckmann, K.W. Zilm, E.K. Paulsen, R.W. Martin, G.T. Montelione, Partial NMR assignments for uniformly (C-13, N-15)-enriched BPTI in the solid state, J. Biomol. NMR 16 (2000) 209–219.

[3] J. Pauli, B. van Rossum, H. Förster, H.J.M. de Groot, H. Oschkinat, Sample optimization and identification of signal patterns of amino acid side chains in 2D RFDR spectra of the α-spectrin SH3 domain, J. Magn. Reson. 143 (2000) 411–416.

[4] J. Pauli, M. Baldus, B. van Rossum, H. de Groot, H. Oschkinat, Backbone and side-chain C-13 and N-15 signal assignments of the α-spectrin SH3 domain by magic angle spinning solid-state NMR at 17.6 tesla, Chem. BioChem. 2 (2001) 272–281.

[5] B.J. van Rossum, F. Castellani, K. Rehbein, J. Pauli, H. Oschkinat, Assignment of the nonexchanging protons of the α-spectrin SH3 domain by two- and three-dimensional H-1–C-13 solid-state magic-angle spinning NMR and comparison of solution and solid-state proton chemical shifts, Chem. BioChem. 2 (2001) 906–914.

[6] L. Duma, A. Lesage, D. Sakellariou, S. Hediger, L. Emsley, Carbon lineshapes in solid-state NMR, in: The 2nd Alpine Conference on Solid-State NMR, Chamonix-Mont Blanc, France, 2001.

[7] A. McDermott, S. Rozovsky, T.I. Igumenova, C.M. Rienstra, A.J. Wand, Studies of proteins by solid-state NMR: insight into catalysis, and the prospects for uniformly labeled systems, in: The 2nd Alpine Conference on Solid-State NMR, Chamonix-Mont Blanc, France, 2001.

[8] M.M. Maricq, J.S. Waugh, NMR in rotating solids, J. Chem. Phys. 70 (1979) 3300–3316.

[9] D.P. Raileigh, M.H. Levitt, R.G. Griffin, Rotational resonance in solid-state NMR, Chem. Phys. Lett. 146 (1988) 71–76.

[10] A.E. Bennett, R.G. Griffin, S. Vega, Recoupling of Homo and Heteronuclear Dipolar Interactions in Rotating Solids, vol. 33, Springer, Berlin, 1994.

[11] T. Nakai, C.A. McDowell, Calculation of rotational resonance NMR spectra using Floquet theory combined with perturbation treatment, Mol. Phys. 88 (1996) 1263–1275.

[12] M.H. Levitt, D.P. Raleigh, F. Creuzet, R.G. Griffin, Theory and simulations of homonuclear spin pair systems in rotating solids, J. Chem. Phys. 92 (1990) 6347–6364.

[13] T. Nakai, C.A. McDowell, Application of Floquet theory to the nuclear-magnetic-resonance spectra of homonuclear 2-spin systems in rotating solids, J. Chem. Phys. 96 (1992) 3452–3466.

[14] R.K. Harris, K.J. Packer, A.M. Thayer, Slow magic-angle rotation C-13 NMR-studies of solid phosphonium iodides—the interplay of dipolar, shielding, and indirect coupling tensors, J. Magn. Reson. 62 (1985) 284–297.

[15] T. Nakai, C.A. McDowell, An analysis of NMR spinning sideband of homonuclear 2-spin systems using Floquet theory, Mol. Phys. 77 (1992) 569–584.

[16] B. Brutscher, Principles and applications of cross-correlated relaxation in biomolecules, Concepts Magn. Reson. 12 (2000) 207–229.

[17] A. Kumar, R.C.R. Grace, P.K. Madhu, Cross-correlations in NMR, Prog. Nucl. Magn. Reson. Spectrosc. 3 (2000) 191–319.

[18] C.J. Hartzell, P.C. Stein, T.J. Lynch, L.G. Werbelow, W.L. Earl, Differential line broadening in the NMR-spectrum of methanol adsorbed on sol–gel silica, J. Am. Chem. Soc. 111 (1989) 5114–5119.

[19] E. Oldfield, F. Adebodun, J. Chung, B. Montez, K.D. Park, H.B. Le, B. Phillips, C-13 nuclear-magnetic-resonance spectroscopy of lipids—differential line broadening due to cross-correlation effects as a probe of membrane-structure, Biochemistry 30 (1991) 11025–11028.

[20] J. Chung, E. Oldfield, A. Thevand, L. Werbelow, A magic-angle sample-spinning nuclear-magnetic-resonance spectroscopic study of interference effects in the nuclear-spin relaxation of polymers, J. Magn. Reson. 100 (1992) 69–81.

[21] E. Oldfield, J. Chung, H.B. Le, T. Bowers, J. Patterson, G.L. Turner, Differential line broadening in coupled C-13 magic-angle sample-spinning nuclear-magnetic-resonance spectra of solid polymers, Macromolecules 25 (1992) 3027–3030.

[22] M.H. Levitt, T.G. Oas, R.G. Griffin, Rotary resonance recoupling in hetero-nuclear spin pair systems, Isr. J. Chem. 28 (1988) 271–282.

[23] T.G. Oas, R.G. Griffin, M.H. Levitt, Rotary resonance recoupling of dipolar interactions in solid-state nuclear magnetic-resonance spectroscopy, J. Chem. Phys. 89 (1988) 692–695.

[24] A. Böckmann, Solid-state NMR sample preparation and ^{13}C assignments of the dimeric form of the HPR like catabolite repression, Poster PB8, in: 16th European Experimental Nuclear Magnetic Resonance Conference, Prague, Czech Republic, 2002, June 9–14.

[25] K.W. Zilm, D.M. Grant, C-13 dipolar spectroscopy of small organic-molecules in argon matrices, J. Am. Chem. Soc. 103 (1981) 2913–2922.

[26] M. Bak, R. Schultz, T. Vosegaard, N.C. Nielsen, Specification and visualization of anisotropic interaction tensors in polypeptides

and numerical simulations in biological solid-state NMR, J. Magn. Reson. 154 (2002) 28–45.
[27] A. Naito, S. Ganapathy, K. Akasaka, C.A. McDowell, Chemical shielding Tensor and C-13–N-14 dipolar splitting in single-crystals of L-Alanine, J. Chem. Phys. 74 (1981) 3190–3197.
[28] C.H. Ye, R.Q. Fu, J.Z. Hu, L. Hou, S.W. Ding, C-13 chemical-shift anisotropies of solid amino-acids, Magn. Reson. Chem. 31 (1993) 699–704.
[29] M.H. Levitt, M. Eden, Numerical simulation of periodic nuclear magnetic resonance problems: fast calculation of carousel averages, Mol. Phys. 95 (1998) 879–890.
[30] C. Filip, S. Hafner, I. Schnell, D.E. Demco, H.W. Spiess, Solid-state nuclear magnetic resonance spectra of dipolar-coupled multi-spin systems under fast magic angle spinning, J. Chem. Phys. 110 (1999) 423–440.
[31] M. Bak, J.T. Rasmussen, N.C. Nielsen, SIMPSON: a general simulation program for solid-state NMR spectroscopy, J. Magn. Reson. 147 (2000) 296–330.
[32] P. Hodgkinson, L. Emsley, Numerical simulation of solid-state NMR experiments, Prog. Nucl. Magn. Reson. Spectrosc. 36 (2000) 201–239.
[33] Matlab, The Mathworks, Inc., Natick, MA.
[34] S.K. Straus, T. Bremi, R.R. Ernst, Resolution enhancement by homonuclear *J* decoupling in solid-state MAS NMR, Chem. Phys. Lett. 262 (1996) 709–715.
[35] T.I. Igumenova, A. McDermott, Homo-nuclear ^{13}C *J*-decoupling in proteins, Poster M/T P 171, in: Experimental Nuclear Magnetic Resonance Conference, Santa Fe, USA, 2002, April 14–19.
[36] F. Ferrage, T.R. Eykyn, G. Bodenhausen, Highly selective excitation in biomolecular NMR by frequency-switched single-transition cross-polarization, J. Am. Chem. Soc. 124 (2002) 2076–2077.
[37] B. Reif, M. Hennig, C. Griesinger, Direct measurement of angles between bond vectors in high-resolution NMR, Science 276 (1997) 1230–1233.
[38] K. Pervushin, R. Riek, G. Wider, K. Wüthrich, Attenuated T-2 relaxation by mutual cancellation of dipole–dipole coupling and chemical shift anisotropy indicates an avenue to NMR structures of very large biological macromolecules in solution, Proc. Natl. Acad. Sci. USA 94 (1997) 12366–12371.
[39] H.J. Simpson, R.E. Marsh, Crystal structure of L-Alanine, Acta Crystallogr. 20 (1966) 550–555.
[40] N. Janes, S. Ganapathy, E. Oldfield, C-13 chemical shielding tensors in L-Threonine, J. Magn. Reson. 54 (1983) 111–121.
[41] D.P. Shoemaker, J. Donohue, V. Schomaker, R.B. Corey, The crystal structure of L-Threonine, J. Am. Chem. Soc. 72 (1950) 2328–2349.
[42] S. Hediger, B.H. Meier, R.R. Ernst, Adiabatic Passage Hartmann–Hahn cross-polarization in NMR under magic-angle sample-spinning, Chem. Phys. Lett. 240 (1995) 449–456.
[43] O.B. Peersen, X.L. Wu, S.O. Smith, Enhancement of CP-MAS signals by variable-amplitude cross-polarization—compensation for inhomogeneous B-1 fields, J. Magn. Reson. Ser. A 106 (1994) 127–131.
[44] S. Hediger, B.H. Meier, N.D. Kurur, G. Bodenhausen, R.R. Ernst, NMR cross-polarization by Adiabatic Passage through the Hartmann–Hahn condition (APHH), Chem. Phys. Lett. 223 (1994) 283–288.
[45] A.E. Bennett, C.M. Rienstra, M. Auger, K.V. Lakshmi, R.G. Griffin, Heteronuclear decoupling in rotating solids, J. Chem. Phys. 103 (1995) 6951–6958.